2512 *Macromolecules* **1995,** *28,* 2512−2518

Synthesis and Nonlinear Optical Characterization of Spin-Coated Films of Triblock Copolymers Containing Durham Polyacetylene

G. S. W. Craig,[†,⊥] **R. E. Cohen,**[*,†] **R. R. Schrock,**[‡] **A. Esser,**[§] **and W. Schrof**[§]

Departments of Chemical Engineering and Chemistry, Massachusetts Institute of Technology, Cambridge, Massachusetts 02139, and BASF AG, ZKM/D−J 542S, D67056 Ludwigshafen, Germany

Received May 4, 1994; Revised Manuscript Received December 19, 1994[⊗]

ABSTRACT: Sequential ring-opening metathesis polymerization of either norbornene or 9-methyltetracyclo[6.2.1.1^{3,6}.0^{2,7}]dodec-4-ene (MTD) and 7,8-bis(trifluoromethyl)tricyclo[4.2.2.0^{2,5}]deca-3,7,9-triene (TCDT) with $\mathrm{Mo(CHCMe_3)(NAr)(OCMe_3)_2}$ (Ar = 2,6-diisopropylphenyl) followed by linking termination with a conjugated dialdehyde results in highly soluble A−B−A triblock copolymers containing a precursor to Durham polyacetylene as the central block. A series of copolymers that contained from 10 to 200 equiv of TCDT was synthesized. The precursor copolymers were spin coated to give submicron thin films. In the case of the copolymers made with norbornene, higher spin speeds resulted in a red shift of the UV/vis spectra of the final polyacetylene-containing copolymer, indicative of longer average conjugation lengths within the film. A red shift was also observed in the UV/vis spectra of copolymers made with more equivalents of TCDT. The nonlinear optical susceptibility ($\chi^{(3)}$) of the copolymers was probed with third harmonic generation and degenerate four-wave mixing. $\chi^{(3)}$ increased with increasing equivalents of TCDT. In all cases, the copolymers made with norbornene had larger $\chi^{(3)}$ values than the copolymers made with MTD.

Introduction

The discovery of the conductivity of doped polyacetylene led to widespread hope that metals and semiconductors could be replaced with conducting polymers. Unfortunately, the same unsubstituted, conjugated p-electron structure of polyacetylene that provided its conductivity also caused the polymer to be extremely oxygen sensitive and intractable, limiting the electronic applicability of polyacetylene. Since the discovery of the conductivity and the undesirable physical properties of polyacetylene, efforts have focused on synthesizing conducting polymers with improved processability, chemically linking conducting polymers with nonconducting, processable polymers, and finding new applications for the unique conjugated electronic structure of conducting polymers like polyacetylene.

In the past decade, the use of conducting polymers in the field of nonlinear optics (NLO) has drawn considerable attention and excitement. The conjugated π-electron structure of conducting polymers results in large NLO coefficients.[1−8] These effects occur in femtosecond time scales because they are electronic in origin. The large NLO coefficients, combined with the ultrafast response time, make conjugated polymers a viable candidate for applications in NLO. Of all of the conducting polymers, oriented polyacetylene has the largest $\chi^{(3)}$.[1]

Research has shown that it is possible to make random[9] and block[10−12] copolymers of Durham polyacetylene and other strained, cyclic olefins such as norbornene. When standard ROMP catalysts were used, such as the $\mathrm{WCl_6/SnMe_3}$ system, only random copolymers were made. It is necessary to use a well-defined metal alkylidene initiator to obtain low-polydispersity block copolymers containing Durham polyacetylene. The block copolymers have better processability than copolymers containing other forms of polyacetylene because the Durham polyacetylene can be kept in its precursor state. As shown by Saunders,[12] the precursor block copolymer can be static cast or spin cast to obtain a variety of block copolymer morphologies. These morphologies also can be oriented. Thermal treatment yields oriented microdomains of polyacetylene in a nonconductive matrix.

To date, the physical and NLO properties of thin films of these copolymers have not been examined. These properties may be of significance because of the large $\chi^{(3)}$ of polyacetylene combined with the utility of spin-coated polymer films. Block copolymers are especially advantageous for the study of NLO properties because the nonconductive block partially isolates the polyacetylene block from other polyacetylene blocks as well as from the atmosphere, thereby increasing the stability of the polyacetylene.

A series of triblock copolymers that contained varying lengths of Durham polyacetylene and nonconductive blocks was prepared. The copolymers were synthesized in a relatively straightforward manner, using ring-opening metathesis polymerization (ROMP) with the Schrock initiator,[13] either norbornene or 9-methyltetracyclo[6.2.1.1^{3,6}.0^{2,7}]dodec-4-ene (MTD), 7,8-bis(trifluoromethyl)tricyclo[4.2.2.0^{2,5}]deca-3,7,9-triene (TCDT), and either hexadienedial or octatrienedial. The precursor block of the triblock copolymers can be converted into polyacetylene in either solution or the solid state.

The precursor triblock copolymers were spin coated into thin films,[14] and the polyacetylene precursor blocks in the copolymer films were converted into Durham polyacetylene. In some cases, the converted copolymers were thermally isomerized. They are characterized with gel permeation chromatography (GPC), and UV/visible

---

[†] Department of Chemical Engineering, Massachusetts Institute of Technology.

[‡] Department of Chemistry, Massachusetts Institute of Technology.

[§] BASF AG.

[⊥] Current address: Raychem Corporate Technology, Menlo Park, CA 94025.

[⊗] Abstract published in *Advance ACS Abstracts,* March 1, 1995.

0024-9297/95/2228-2512$09.00/0

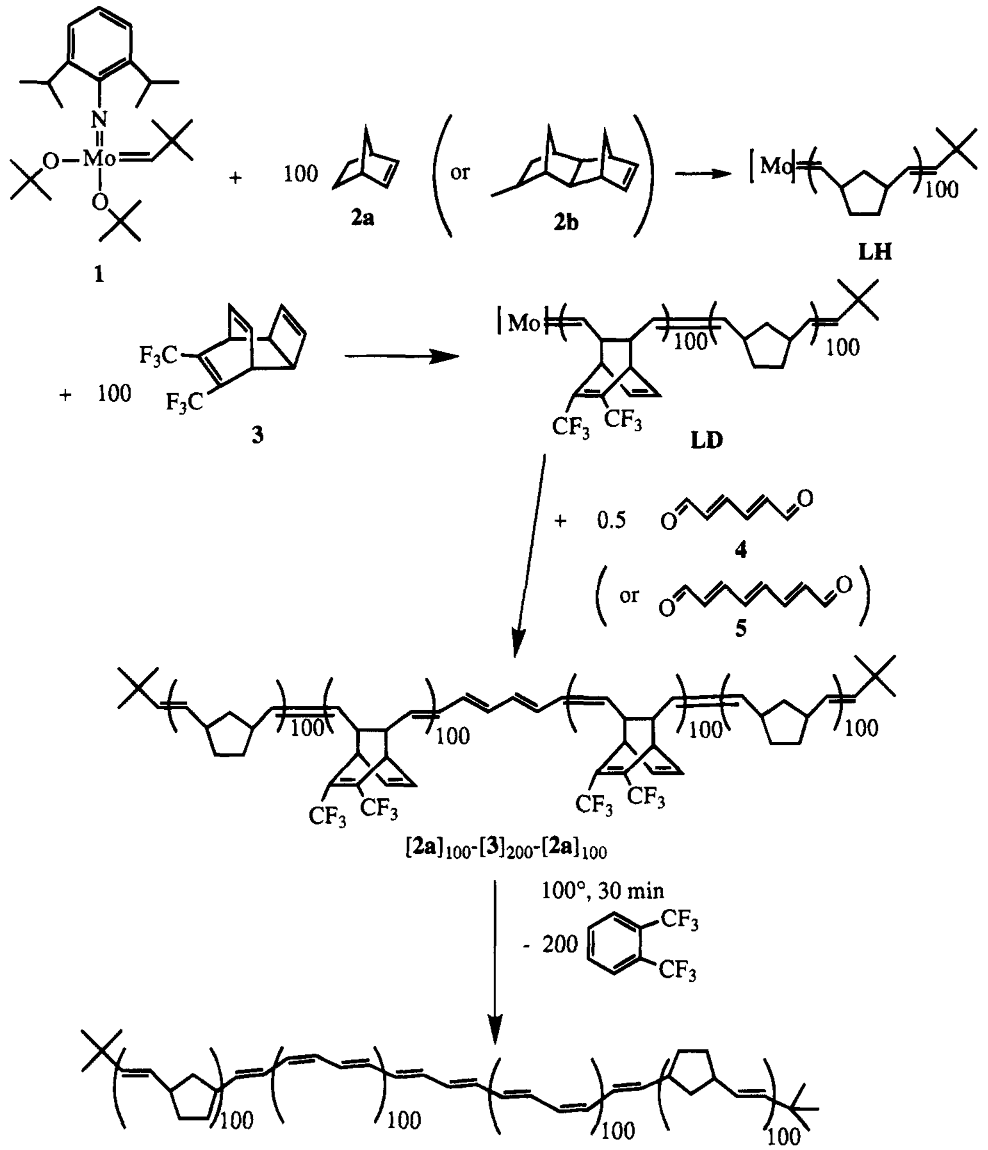

Figure 1. Example linking copolymerization route to triblock copolymer $[\mathbf{2a}]_{100}$–$[\text{ene}]_{400}$–$[\mathbf{2a}]_{100}$.

spectroscopy (UV/vis). The NLO properties of the copolymers were analyzed with third harmonic generation (THG) and degenerate four-wave mixing (DFWM).

Copolymer Synthesis

General Procedures. All syntheses were performed under a nitrogen atmosphere in either a Vacuum Atmospheres or an Innovative Technologies drybox or by using standard Schlenk/vacuum line techniques. Tetrahydrofuran (THF) was degassed, stirred over sodium/potassium alloy (Na/K) until the solvent turned blue, and then vacuum transferred immediately before use. Toluene for polymerizations was distilled over sodium, then stored over Na/K under nitrogen, and filtered and degassed prior to use. Methylene chloride was distilled from calcium hydride and stored over molecular sieves. Pivaldehyde was distilled twice from calcium hydride, degassed, and stored under nitrogen at −40° C. Norbornene (**2a**) was purified by distillation over sodium. 9-Methyltetracyclo[6.2.1.1^{3,6}.0^{2,7}]dodec-4-ene (**2b**) was vacuum distilled over sodium and stored under nitrogen. Mo(CHCMe$_3$)(NAr)(OCMe$_3$)$_2$ (Ar = 2,6-diisopropylphenyl) (**1**),[18] 7,8-bis(trifluoromethyl)tricyclo[4.2.2.0^{2,5}]deca-3,7,9-triene (**3**),[19] hexa-2,4-diene-1,6-dial (**4**),[20] and octa-2,4,6-triene-1,8-dial (**5**)[21,22] were synthesized according to literature procedures.

Synthetic Methods. All polymers were synthesized by ring-opening metathesis polymerization (ROMP) using initiator **1**. This initiator has been shown to yield homopolymers of **2a** that have a very narrow molecular weight distribution.[13] **2a** and **2b** were used to examine the effects of T_g of the nonconjugated blocks on polyacetylene. Poly(**2a**) has a T_g of roughly 35 °C whereas poly(**2b**) has a T_g of approximately 205 °C.[23] The polyene precursor monomer **3** was used because it was sufficiently stable at room temperature, it quickly converted to polyacetylene under mild conditions (100 °C, 30 min), and it was easy to synthesize relative to other Durham polyacetylene precursor monomers.

The copolymers studied here all have the same precursor structure: $[\mathbf{2}]_x$–$[\mathbf{3}]_y$–$[\mathbf{2}]_x$. **2** represents either norbornene (**2a**) or methyltetracyclododecene (**2b**). The subscripts x and y ranged from 50 to 100 and from 10 to 200, respectively. The subscript refers to the number of equivalents added during the polymerization; the actual block lengths may vary. Conversion of the polyacetylene precursor block yields two double bonds per equivalent of **3**, as shown in Figure 1. After conversion of the polyacetylene precursor block, the copolymers are identified by $[\mathbf{2}]_x$–$[\text{ene}]_{2y}$–$[\mathbf{2}]_x$. In this case, the subscript $2y$ refers to the number of double bonds in the center block, but not the number of double bonds in conjugation in the center block.

The linking copolymerization of $[\mathbf{2a}]_{100}$–$[\mathbf{3}]_{200}$–$[\mathbf{2a}]_{100}$ and conversion to $[\mathbf{2a}]_{100}$–$[\text{ene}]_{400}$–$[\mathbf{2a}]_{100}$, diagrammed in Figure 1, is presented as an example of the polymerization technique. A solution of **1** (26 mg, 0.053 mmol) in 2 mL of toluene was injected into a solution of **2a** (0.5 g, 5.31 mmol) in 40 mL of toluene at room temperature, and the mixture was stirred for

5 min to form the living homopolymer **LH**. A solution of **3** (1.41 g, 5.31 mmol) in 5 mL of toluene was added to the **LH** solution and stirred for 25 min to form the living diblock copolymer **LD**. The linking termination was accomplished by adding a solution of **4** (2.92 mg, 0.027 mmol) in 2 mL of toluene to the **LD** solution and stirring for 25 min. (The choice of the linking agent, either **4** or **5**, for any given polymerization was arbitrary. The length of the polyacetylene sequences made the difference of one extra double bond inconsequential.) Finally, to drive the linking reaction to completion, the solvent was removed under vacuum. The resulting precursor copolymer $[\mathbf{2a}]_{100}-[\mathbf{3}]_{200}-[\mathbf{2a}]_{100}$ was dissolved in 10 mL of methylene chloride. Initiator residue was removed by precipitating the polymer by dropwise addition of the methylene chloride solution to cold methanol. The polymer was collected on a Millipore 10 μm filter on a glass frit, washed with cold methanol, and dried under vacuum.

Films of the precursor were prepared by spin coating or by static casting. In the case of spin coating, solutions of 1−10 wt % of precursor copolymer in toluene were spin coated onto microscope slides with a Headway Research spin coater. The solutions were deposited onto the substrate while it was motionless, as recommended in the literature.[17] The samples were spin coated in the drybox. The films were spin coated at speeds ranging from 1500 to 8000 rpm for 60 s. In the case of homopolymers of **3**, THF was used instead of toluene.

Static cast samples were prepared from either pure triblock copolymer or from a 50:1 homopolymer:triblock copolymer blend. The films made from blends were used primarily in the UV/vis characterization of the triblock copolymers. The dilution of the copolymer in the homopolymer served two functions. First, it reduced the absorption intensity of the films, which were very thick relative to the spin-coated films. Second, the homopolymer provided a constant dielectric matrix for the UV/vis analysis. If the UV/vis analysis of wavelength of absorption as a function of equivalents of **3** was performed on films of pure triblock copolymer, the measurements would be convoluted by changes in the bulk dielectric coefficient of the copolymer as the equivalents of **3** changed. Films were static cast in the drybox from ~8 wt % solutions of polymer blend in either methylene chloride, THF, or toluene. The films were cast onto glass microscope slides. The glass slide was bordered with Teflon-coated aluminum foil to keep the polymer solution on the glass slide.

Regardless of the film preparation technique used, the precursor copolymers were converted to the polyacetylene-containing copolymers in the solid state. In the case of $[\mathbf{2a}]_{100}-[\mathbf{3}]_{200}-[\mathbf{2a}]_{100}$, the polymer is converted to $[\mathbf{2a}]_{100}-[\text{ene}]_{400}-[\mathbf{2a}]_{100}$. After thermal conversion, the polyacetylene block is in an alternating *trans(cistrans)*$_x$ isomeric state, with the exception of the two (or three if linking agent **5** is used) central *trans* double bonds. The polyacetylene block was thermally converted to the *all-trans* isomer by heating the film at 150 °C for 30 min in the same apparatus in which the precursor polymer was converted.

Copolymer Characterization

Experimental Apparatus. Gel permeation chromatographic (GPC) analysis was carried out at room temperature employing a Rheodyne Model 7125 sample injector, a Kratos Spectroflow 400 pump, Shodex KF-802.5, 803, 804, 805, and 800P columns, a Knauer differential refractometer, and a Spectroflow 757 absorbance detector. Solutions were 0.1−0.3% w/v in THF and were filtered through a Millex-SR 0.5 μm filter in order to remove particulates. The GPC columns were calibrated using commercially available polystyrene standards (Polymer Laboratories Ltd.) ranging from 1206 to 1.03×10^6 g/mol. Molecular weights (M_n) quoted here represent the molecular weight of a polystyrene standard that would elute in the same volume element as the polymer under consideration.

The UV/vis spectra of the films were measured at room temperature on a Hewlett-Packard 8452A in-line diode array spectrophotometer. The IR spectra were taken on a Perkin-Elmer 1420 ratio recording infrared spectrometer. Scan times of 12 or 48 min were used. The baseline transmittance was set at 90% for each scan. Precursor polymer films were static cast on KBr plates, converted to polyacetylene, and isomerized as described in the synthesis section.

Nonlinear Optical Analysis. THG and DFWM[8] techniques were used for measurements of the third-order polarizabilities. The THG experiment is based on the Maker fringe method. Frequency-tunable light pulses were generated by an optical parametric oscillator (OPO, GWU Lasertechnik) which was pumped by a frequency-tripled, Q-switched Nd:YAG laser (Lumonics HyperYag 1200). The pump laser operates at a repetition rate of 20 Hz with a pulse duration of 7 ns. The pulse length is further shortened to about 4 ns by the parametric generation process. The idler wavelengths of the OPO can be tuned from 700 to 2500 nm. In all measurements the maximum pulse energy impinging onto the sample does not exceed 2 mJ.

The sample was mounted on a computer-controlled rotary stage within a vacuum cell to avoid THG contributions from air and to minimize sample degradation. The fundamental beam was focused onto the sample with a 30 cm focal length lens. The THG signal was detected and measured by a monochromator, photomultiplier tube, and a fast oscilloscope (HP-545 10A). In order to compensate for the fluctuations of the OPO intensity, a reference (quartz) THG measurement was run simultaneously.

DFWM measurements were performed in the "folded boxcar" configuration using 100 fs light pulses derived from a mode-locked Ti:sapphire laser (Coherent Mira900F). With the short-wave mirror set of the Ti:sapphire laser it was possible to tune the wavelength of the pulses in the range between 715 and 820 nm. The output beam of the Ti:sapphire laser was split into three partial beams by two beam splitters. Two of the three beams were used for the generation of a refractive index grating in the sample, while the third beam was used for the detection of this grating, i.e., the light-induced change of the refractive index. In order to synchronize all pulses in time, two of the three beams were fed into computer-controlled delay stages. The three collinear beams were focused onto the sample spot by a lens of a focal length of 100 mm, leading to a focal diameter of approximately 20 μm. The deflected beam, e.g., the DFWM signal, was detected by a photomultiplier (Hamamatsu R298) after passing a spatial filter. Lock-in techniques were used to improve the signal to noise ratio of the DFWM signal. Therefore two of the incoming beams were chopped by a mechanical chopper at different frequencies (f_1 and f_2). The DFWM signal from the multiplier was fed into a lock-in amplifier (Stanford Research SR530) referenced at the sum frequency ($f_1 + f_2$). The maximum amplitude of the diffracted signal observed around zero time delay (see Figure 9) in all materials investigated in this study was compared to the maximum amplitude in a reference sample under identical experimental conditions. As a reference, CS_2 in a quartz cuvette of 1 mm thickness was used.

Results

Polymerization and Isomerization. Triblock copolymers of **2a** and **3** synthesized by linking ROMP with **1** have been reported previously.[24] As in the case of the triblock copolymers containing polyenes, the linking step in the copolymerization did not have a detrimental effect on the polydispersity of the copolymers. Substitution of **2b** for **2a** in the polymerization was straightforward. Copolymers containing **2b** and **3** precipitated from methanol more readily than those containing **2a** and **3**.

The GPC scan of most of the copolymers consisted of one peak with negligible shoulders. Occasionally a double molecular weight shoulder appeared, as in Figure 2. The molecular weight doubling was caused by oxygen contamination as discussed in detail elsewhere.[12] The GPC scans of polymers that had different block lengths varied as expected. For example, the

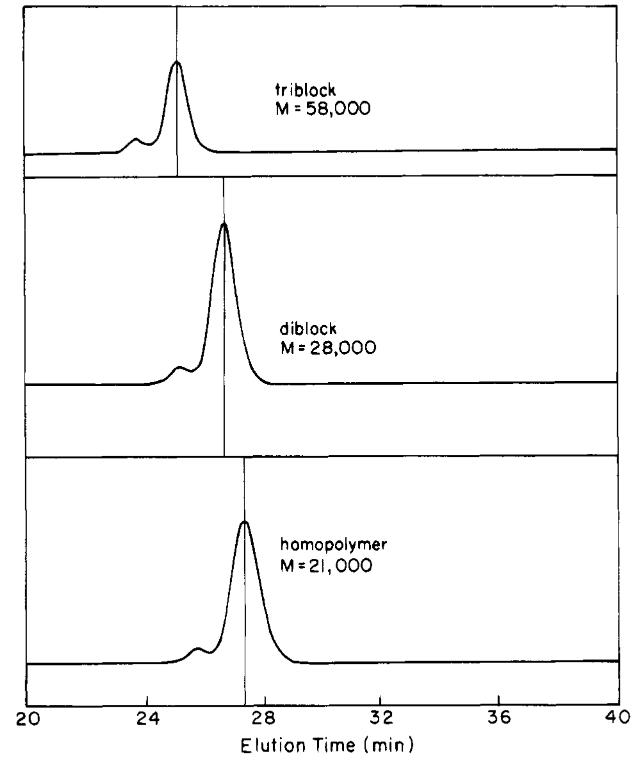

Figure 2. GPC scans of $[\mathbf{2a}]_{100}$, $[\mathbf{2a}]_{100}-[\mathbf{3}]_{30}$ and $[\mathbf{2a}]_{100}-[\mathbf{3}]_{30}-[\mathbf{2a}]_{100}$.

precursor to $[\mathbf{2a}]_{100}-[\mathbf{3}]_{100}-[\mathbf{2a}]_{100}$ eluted before the precursor to $[\mathbf{2a}]_{100}-[\mathbf{3}]_{40}-[\mathbf{2a}]_{100}$. During some of the polymerizations, aliquots were taken at each step to monitor the progression of the polymerization by GPC. The progression from living homopolymer $[\mathbf{2a}]_{100}$ to living diblock copolymer $[\mathbf{2a}]_{100}-[\mathbf{3}]_{200}$ to $[\mathbf{2a}]_{100}-[\mathbf{3}]_{200}-[\mathbf{2a}]_{100}$ is presented in Figure 2. The polydispersity of the triblock copolymers ranged from 1.05 to 1.20.

The solid-state thermal conversion process was followed visually. Initially, the polymer films were clear or light yellow. After the first few minutes of heating, all of the copolymers became red. After prolonged heating, all of the copolymers that contained norbornene were purple except the ones containing only 20 equiv of **3**. The copolymers that contained MTD turned red or reddish-purple. In all cases, as the amount of **3** in the polymer increased, the converted copolymer became more reflective. In the case of homopolymers of **3**, the converted polymer, Durham polyacetylene, was as reflective as a polished silicon wafer.

UV/vis Spectroscopy. The UV/vis spectra of the triblock copolymers containing polyacetylene consisted of a broad envelope with a maximum absorption wavelength, $\lambda_{\max}$, in the 500–590 nm range. There were no vibronic fingers similar to those which appear in the spectra of triblock copolymers containing polyenes.[24] Isomerization of the polyacetylene did not have a noticeable effect on the UV/vis spectra. A typical spectrum is shown in Figure 3.

As shown previously for polyenes,[24,25] E_N, the energy of absorption of an N-ene, is inversely related to the conjugation length N:

$$E_N = \frac{hc}{\lambda_{\max}} = E_\infty + \frac{k}{N} \qquad (1)$$

where h is Planck's constant, c is the speed of light, E_∞ is the absorption energy of a hypothetical, infinite polyene, and k is a constant. The relationship in eq 1 is used in Figure 4 to show the effect of additional equivalents of **3** on the UV/vis spectra of the block copolymers. Specifically, the $\lambda_{\max}$ values of the static cast block copolymer/homopolymer blends are presented in terms of energy of absorption versus nominal conjugation length. The nominal conjugation length is simply twice the number of equivalents of **3** in the polymer. The triblock copolymers synthesized with more equivalents of **3** had larger values of $\lambda_{\max}$. As expected, the $\lambda_{\max}$ values for these copolymers containing polyacetylene did not follow the trend shown in Figure 4 for previously studied copolymers containing short polyene sequences.[24] The conjugation lengths exhibited in this work were significantly smaller than the nominal conjugation lengths. The actual conjugation length depended on the length and type of the **2a** and **2b** and could be manipulated by processing steps as described in the next section.

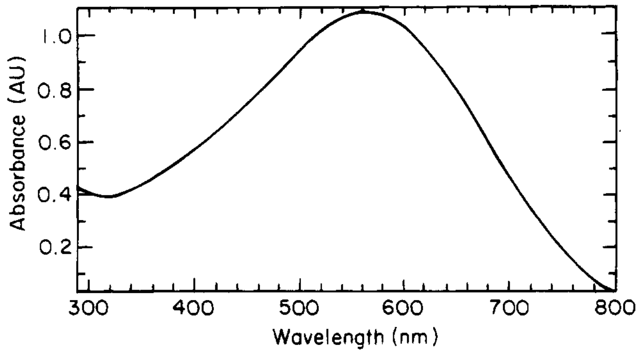

Figure 3. UV/vis spectrum of static cast $[\mathbf{2a}]_{100}-[\mathrm{ene}]_{100}-[\mathbf{2a}]_{100}$.

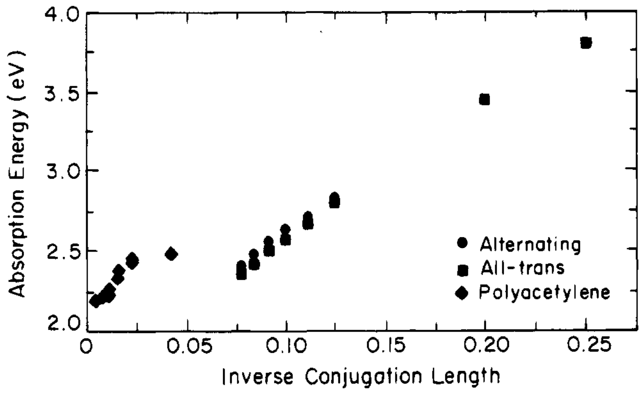

Figure 4. Absorption energy of static cast triblock copolymers containing alternating polyacetylenes, alternating polyenes, and *all-trans* polyenes.[24] A nominal conjugation length was used for the polyacetylene data, corresponding to twice the number of equivalents of **3** in the polymer.

Effect of Spin Coating. Orientation of polymer chains has been observed previously in spin-coated films.[26] For some of our spin-coated films of triblock copolymers there is evidence of chain orientation that is dependent on spin speed. The extent of chain orientation was inferred from the $\lambda_{\max}$ of the UV/vis spectra. The dependence of $\lambda_{\max}$ on speed is shown in Figure 5.

It is possible to use a fit of eq 1 to the previously measured polyene data[24] in Figure 4 to calculate a conjugation length for each copolymer sample in this study after it has been processed either by static casting or spin coating. The degree to which spin speed influenced the observed value of conjugation length, i.e., N calculated from eq 1, is shown in Figure 6. The

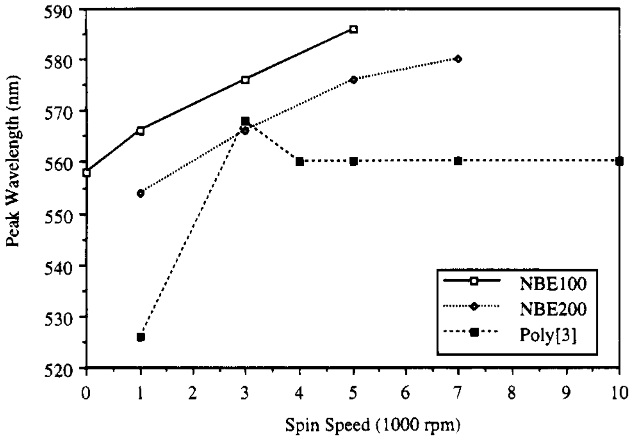

Figure 5. Variation of λ_{max} with spin speed in spin-coated films of polyacetylene homopolymer and of polynorbornene–polyacetylene–polynorbornene triblock copolymers. λ_{max} values corresponding to spin speeds of 0 rpm were determined from static cast films. The lines are included to aid the eye in viewing the data.

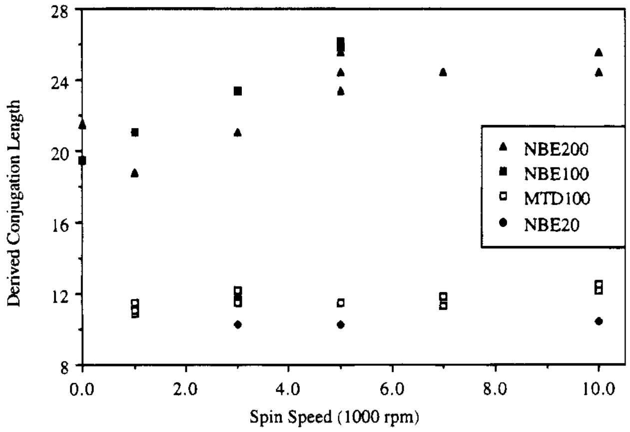

Figure 6. Effect of spin speed on effective conjugation length of triblock copolymers containing **3** and either norbornene or MTD. Effective conjugation length was derived from the fit of eq 1 to the polyene data in Figure 4.

Table 1. $\chi^{(3)}$ Values of Triblock Copolymers (Units of 10^{-12} esu)

	$[\mathbf{2a}]_{100}-[\text{ene}]_n-[\mathbf{2a}]_{100}$				$[\mathbf{2b}]_{100}-[\text{ene}]_n-[\mathbf{2b}]_{100}$		
	$n =$ 20	$n =$ 100	$n =$ 200	$n =$ 400	$n =$ 100	$n =$ 200	$n =$ 400
THG 1650 nm	2.6	60	200	320	32	90	220
THG 1650 nm *all-trans*	3.1	53	220	310	28	60	200
THG 1900 nm		50	180	250	18	18	52
THG 1900 nm *all-trans*		32	120	150			
DFWM 715 nm	160	3800	11000	13000	1000	1500	2200
DFWM 715 nm *all-trans*	400	3200	9000	12000	430	1000	2700

dependence of conjugation length on spin speed was not observed in $[\mathbf{2a}]_{100}-[\text{ene}]_{20}-[\mathbf{2a}]_{100}$, which has the shortest length of polyacetylene block of the copolymers in this study. There was no reliable trend for the influence of spin speed on the triblock copolymers containing blocks of poly(**2b**) and for the homopolymers of poly(**3**).

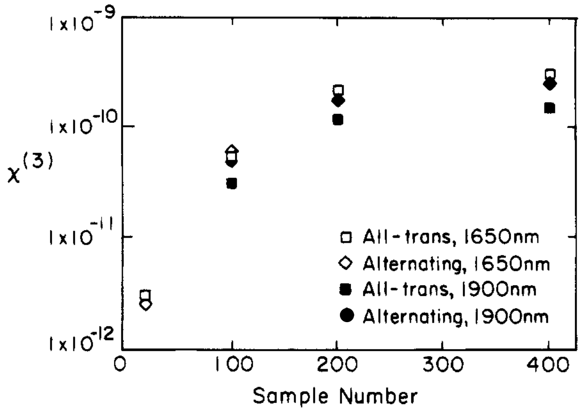

Figure 7. THG measurements of polynorbornene–polyacetylene–polynorbornene triblock copolymers at 1650 and 1900 nm for both the alternating and the *all–trans* isomers.

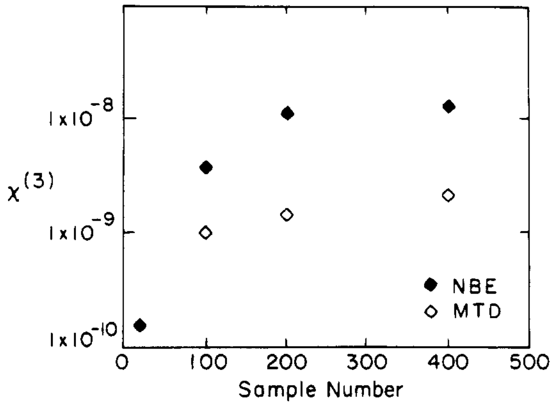

Figure 8. DFWM results for copolymers containing polynorbornene and copolymers containing poly(MTD).

Nonlinear Optical Results. The results of the NLO measurements are listed in Table 1. As shown in Figure 7, there was only a slight increase in $\chi^{(3)}(-3\omega;\omega,\omega,\omega)$ at 1.65 μm compared to 1.90 μm. Isomerization of the polyacetylene to *all-trans* led to slightly lower values of $\chi^{(3)}$. The difference in $\chi^{(3)}$ of the triblock copolymers containing polynorbornene versus those containing poly(MTD) is shown in Figure 8. This difference was observed in both the THG and DFWM measurements. The DFWM measurements revealed an ultrafast response time, on the order of 1 picosecond, for the polyacetylene, as shown in Figure 9.

Resonance enhancement was observed in the DFWM measurements as the fundamental wavelength was decreased, as shown in Figure 10. $\chi^{(3)}(-\omega;\omega,-\omega,\omega)$ remained fairly constant from 806 to 726 nm. At 715 nm, a significant increase in $\chi^{(3)}$ occurred. The resonance behavior was observed for both the alternating and *all-trans* isomer of $[\mathbf{2a}]_{100}-[\text{ene}]_{100}-[\mathbf{2a}]_{100}$.

Discussion

Polymerization and Isomerization. The polymerization of the triblock copolymers of **2a** or **2b** and **3** was identical to the previously studied linking copolymerization of triblock copolymers containing polyenes.[24] The only difference was the extra equivalents of **3** that were needed to generate the long polyacetylene sequences instead of short polyenes. The linking polymerization route worked very well when the appropriate stoichiometry of dialdehyde was used.

Exact molecular weights of the copolymers could not be determined from GPC because of the lack of an

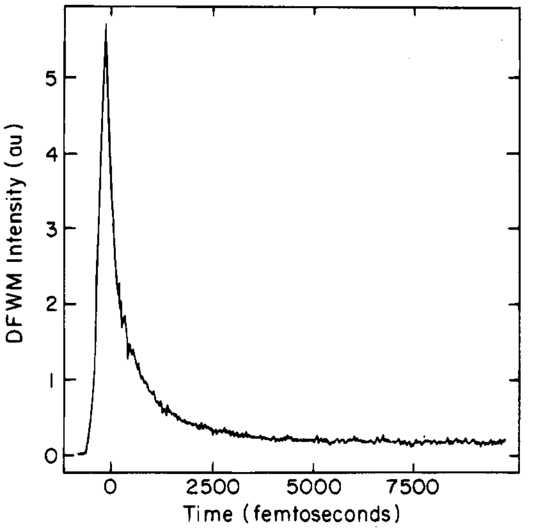

Figure 9. Temporal response of DFWM measurements on $[\mathbf{2a}]_{100}-[\text{ene}]_{100}-[\mathbf{2a}]_{100}$.

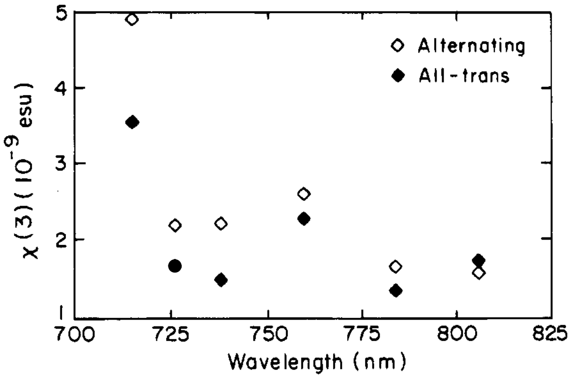

Figure 10. DFWM spectra of $[\mathbf{2a}]_{100}-[\text{ene}]_{100}-[\mathbf{2a}]_{100}$ before and after isomerization.

appropriate polystyrene/poly(**2**)–poly(**3**)–poly(**2**) conversion factor. Such a conversion factor would be difficult to calculate because of the different chain characteristics of the blocks, as well as the variation in the desired length of the middle block. The double molecular weight peak apparent in the GPC scans in Figure 2 was caused by oxygen contamination.[12] This peak was eliminated by degassing the polymerization solvent immediately before the polymerization.

UV/vis Spectroscopy. As expected, the linear fit previously derived for short polyenes could not be extrapolated to include the λ_{max} values of the triblock copolymers containing polyacetylenes of this work. The λ_{max} values of the triblock copolymers were smaller than extrapolation of the linear fit would predict. The lower values of λ_{max} most likely resulted from a combination of cross-linking and kinks in the polyacetylene backbone. The λ_{max} values of the triblock copolymers did increase with increasing equivalents of **3**, similar to the previous work on short polyenes. It should be noted that the increase in the λ_{max} could not be due to changes in the dielectric coefficient of the media because the solvent, poly(**2a**) homopolymer, was the same in all cases shown in Figure 4.

The increase in λ_{max} across the entire range of nominal conjugation lengths was unexpected. The increase reflects a corresponding increase in the average conjugation length with increasing equivalents of **3**. In a given triblock copolymer containing polyacetylene, the probability of achieving any particular conjugation length is determined by a variety of factors, including steric hindrance, cross-linking, chain orientation, and chain entanglement. One would expect that these factors should approach an asymptotic limit, such that the number of equivalents of **3** in the middle block no longer affects the λ_{max} of the spectrum. As shown in Figure 4, an asymptotic limit in λ_{max} as a function of equivalents of **3** was not observed even when 200 equiv of **3**, corresponding to 400 double bonds, was used.

There are at least two possible reasons for the observed increase in λ_{max}. First, the conjugation length of the polyacetylene may be limited by the amount of **3** originally incorporated in the polymer. If the extremely long conjugation lengths associated with absorbances at long wavelengths are not present in the material, the entire envelope will be shifted to shorter wavelengths, resulting in a smaller λ_{max}.

Stress-induced orientation caused by volume reduction during the conversion to polyacetylene is another plausible explanation for the dependence of λ_{max} on the number of repeat units of **3**. A decrease in molar volume occurs during the conversion from poly(**3**) to polyacetylene because of the loss of hexafluoroxylene. Previous studies on Durham polyacetylene have concluded that this volume change causes a significant stress field on the polymer that results in the orientation of the polymer chain.[27] The copolymers that have a longer block of **3** have a greater decrease in volume during the conversion. The larger loss of volume causes more stress on the sample, possibly resulting in greater orientation of the polyacetylene chains and extension of the conjugation.

Support for the volume reduction hypothesis may come from a comparison of the copolymer made with norbornene versus with MTD. The MTD triblocks have a smaller λ_{max} than the norbornene triblocks. Poly(MTD) is a high-T_g material that remains glassy during the conversion process and therefore would not deform under the stress induced by the volume reduction process. Polynorbornene on the other hand is a low-T_g material that could permit the polyacetylene chains to orient during conversion.

Effect of Spin Coating. The noticeable effect of spin speed on λ_{max} suggests that any orientation caused by spinning must carry through the conversion from poly(**3**) to polyacetylene in order to affect the conjugation in the final polyacetylene chain. This effect occurred only in the copolymers that contained polynorbornene. It is likely that there is enough solvent present in the low-T_g polynorbornene in the final stages of the spin-coating process for the polynorbornene blocks to behave like a fluid and allow the copolymers to orient at ambient temperature. Conversely, the T_g of poly(MTD) in the final stages of spin coating will be much higher than ambient temperature even if the T_g is slightly reduced due to the presence of solvent. The poly(MTD) blocks will not have liquid properties and this will inhibit any orientation of the MTD-containing copolymers.

The lack of conclusive evidence that spin speed affects the effective conjugation length of homopolymers of poly(**3**) suggests that the polynorbornene blocks are necessary for the enhancement of the effective conjugation length. Also, a sufficient length of poly(**3**) is evidently necessary for the effect because no increase in the effective conjugation length of $[\mathbf{2a}]_{100}-[\text{ene}]_{20}-[\mathbf{2a}]_{100}$ was observed with increasing spin speed.

Nonlinear Optical Results. Although detailed quantitative conclusions cannot be drawn from the NLO measurements because of a limited amount of sample degradation, the qualitative trends observed in Table 1 and Figures 7–10 are clear. The fact that thermal isomerization of the samples resulted in a decrease of $\chi^{(3)}$ suggests that degradation occurred during isomerization. This conclusion is supported by the UV/vis analysis of the copolymers.

Our results show that the NLO properties depended strongly on factors not normally associated with NLO activity. The triblock copolymers containing polynorbornene had larger NLO coefficients than those containing poly(MTD). The larger $\chi^{(3)}$ values of the polynorbornene copolymers, as well as the higher values of $\lambda_{\max}$, suggest that relatively facile processing conditions can affect the effective conjugation lengths of the polyacetylene sequences in these copolymers. As expected, the longer effective conjugation length also led to an increase of $\chi^{(3)}$ as the nominal number of double bonds (e.g., "200" for $[\mathbf{2a}]_{100}$–$[\mathrm{ene}]_{200}$–$[\mathbf{2a}]_{100}$) was increased.

Resonance enhancement of $\chi^{(3)}$ is expected and has been observed previously in polyacetylene.[8] The resonance enhancement was seen in both the DFWM and the THG measurements when they were repeated at shorter wavelengths. The picosecond response time and large $\chi^{(3)}$ of the copolymers also duplicate previous NLO studies on polyacetylene.

Conclusions can also be drawn from the rates of degradation of the triblock copolymers containing Durham polyacetylene and the homopolymers of Durham polyacetylene. Our methods of sample handling exposed the samples to subambient concentrations of oxgyen. Under this low level of oxygen contamination, the purple films of Durham polyacetylene homopolymer degraded to an almost colorless material within 1 week. The films of all of the triblock copolymers degraded much less rapidly than the Durham polyacetylene homopolymer films. The triblock copolymers containing polynorbornene were the most noticeably stable. These samples retained a large $\chi^{(3)}$ and a purple color over the same period of time (about 2 weeks) that the copolymers containing poly(MTD) turned yellow. The presence of the poly(MTD) or polynorbornene decreases the oxygen sensitivity of the polyacetylene because the oxygen has less access to the polyacetylene chains. In the case of polynorbornene, the oxygen stability may be enhanced further because of lower oxygen solubility in a low-T_g material compared to a high-T_g analog.[28]

Conclusion

The sequential polymerization of either **2a** or **2b** and **3** with the Schrock initiator **1** followed by linking termination with a dialdehyde yielded low-polydispersity triblock copolymers. The poly(**3**) block could be thermally converted to polyacetylene and isomerized. The precursor block copolymers were highly soluble and produced quality thin films when spin coated from toluene solution. After conversion, the films were red or purple. These films had very large $\chi^{(3)}$ values and ultrafast NLO response times. The $\chi^{(3)}$ values depended on the conjugation length extension of the polyacetylene block and by the choice of polynorbornene or poly(MTD) for the companion block sequences. As shown in the UV/vis spectra, the polyacetylene conjugation length can be extended either by addition of more of monomer **3** or, in the case of polynorbornene–polyacetylene–polynorbornene triblock copolymers, by spin coating at higher spin speeds.

The NLO properties of polyacetylene have been studied in detail previously,[1,7,8] and the results presented here are similar. The unique feature of the triblock copolymers containing Durham polyacetylene is that they have approximately the same NLO properties as the polyacetylene homopolymers, but they are much more stable and tractable. The precursor copolymer can be refrigerated and stored under nitrogen almost indefinitely without detrimental effects to its final NLO properties. When desired, the copolymer can be spin coated into high-quality, micron-thin films, converted into triblock copolymers containing polyacetylene, and used.

Acknowledgment. The MIT authors thank the National Science Foundation (Grant DMR 87-19217 through the MIT Center for Materials Science and Engineering) for support of this research. Funding of the Industrial Science and Technology Frontier Program supported by the New Energy and Industrial Technology Development Organization (NEDO, Japan) is gratefully acknowledged by BASF AG.

References and Notes

(1) Drury, M. R. *Solid State Commun.* **1988**, *68*, 417.
(2) Sinclair, M.; McBranch, D.; Moses, D.; Heeger, A. J. *Synth. Met.* **1989**, *28*, D645.
(3) Fann, W. S.; Benson, S.; Madey, J. M. J.; Etemad, S.; Baker, G. L.; Kajzar, F. *Phys. Rev. Lett.* **1989**, *62*, 1492.
(4) Krausz, F.; Wintner, E.; Leising, G. *Phys. Rev. B* **1989**, *39*, 3701.
(5) Kanetake, T.; Ishikawa, K.; Hasegawa, T.; Koda, T.; Takeda, K.; Hasegawa, M.; Kubodera, K.; Kobayashi, H. *Appl. Phys. Lett.* **1989**, *54*, 2287.
(6) Zhao, M. T.; Singh, B. P.; Prasad, P. N. *J. Chem. Phys.* **1988**, *89*, 5535.
(7) Worland, R.; Phillips, S. D.; Walker, W. C.; Heeger, A. J. *Synth. Met.* **1989**, *28*, D663.
(8) Prasad, P. N.; Williams, D. J. *Introduction to Nonlinear Optical Effects in Molecules and Polymers*, 1st ed.; John Wiley and Sons, Inc.: New York, 1991.
(9) Ramakrishnan, S.; Hirsch, J. A.; Martinez, J. R.; Chien, J. C. W. *J. Polym. Sci., Polym. Chem. Ed.* **1989**, *27*, 3937.
(10) Krouse, S. A.; Schrock, R. R. *Macromolecules* **1988**, *21*, 1885.
(11) Stelzer, F.; Grubbs, R. H.; Leising, G. *Polymer* **1991**, *32*, 1851.
(12) Saunders, R. S. Ph.D. Thesis, Massachusetts Institute of Technology, 1992; *Macromolecules* **1992**, *24*, 5599.
(13) Schrock, R. R. *Acc. Chem. Res.* **1990**, *24*, 158.
(14) Scriven, L. E. In *Better Ceramics Through Chemistry III*; Materials Research Society: Boston, 1988; p 717.
(15) Lawrence, C. J. *Phys. Fluids* **1988**, *31*, 2786.
(16) Spangler, L. L.; Torkelson, J. M.; Royal, J. S. *Polym. Eng. Sci.* **1990**, *30*, 644.
(17) Daughton, W. J.; Givens, F. L. *J. Electrochem. Soc.* **1979**, *126*, 269.
(18) Schrock, R. R.; Murdzek, J. S.; Bazan, G. C.; Robbins, J.; DiMare, M.; O'Regan, M. *J. Am. Chem. Soc.* **1990**, *112*, 3875.
(19) Bursics, A. R. L.; Bursics-Szekeres, E.; Murray, M.; Stone, F. G. A. *J. Fluorine Chem.* **1975**, *7*, 619.
(20) Kossmehl, G.; Bohn, B. *Chem. Ber.* **1974**, *107*, 710.
(21) Cope, A. C.; Nelson, N. A.; Smith, D. A. *J. Am. Chem. Soc.* **1954**, *76*, 1100.
(22) Anet, R. *Tetrahedron Lett.* **1961**, *20*, 720.
(23) Schneider, W. U.S. Patent 4 320 239, 1982.
(24) Craig, G. S. W.; Cohen, R. E.; Schrock, R. R.; Silbey, R. J.; Puccetti, G.; Ledoux, I.; Zyss, J. *J. Am. Chem. Soc.* **1993**, *115*, 860.
(25) Knoll, K.; Schrock, R. R. *J. Am. Chem. Soc.* **1989**, *111*, 7989.
(26) Prest, W. M. J.; Luca, D. J. *J. Appl. Phys.* **1979**, *50*, 6067.
(27) Lugli, G.; Pedretti, U.; Perego, G. *Mol. Cryst. Liq. Cryst.* **1985**, *117*, 43.
(28) Rein, D. H.; Baddour, R. F.; Cohen, R. E. *Polymer* **1992**, *33*, 1696.

MA9460044